BANG, BANG, BEEP - NON-OPERATIONAL AIRBORNE SOUND FROM OFFSHORE WINDFARMS

A Leiper SSE Renewables, Inverness, Scotland

1 INTRODUCTION

Offshore wind is expected to undergo significant growth in the coming years, both in the UK[1] and internationally[2]. While there has been a trend for increased distance from the shore[3], this is not universal, with some markets seeing significant growth relatively close to the shore[4,5].

Operational offshore turbine sound power level data are increasingly being made available, even if not publicly, and Denmark has introduced a calculation procedure for the calculation of noise from offshore wind turbines[6]. However, there has been relatively little new information or research into airborne sound associated with piling[7], despite the trend of significantly larger piles and hammer energies. In addition, the effects of noise from fog signals, which are required to be installed in the UK[8], is an overlooked area. These topics are explored in this paper.

2 OFFSHORE PILING

2.1 Introduction

In comparison with underwater noise from piling, which has seen increased research in recent years, there is a paucity of information relating to the airborne sound from offshore piling[7]. This is in spite of the fact that offshore piling sound has been distinctively measured at distances of 15 – 20 km[9] and that there have been high profile noise complaints relating to night time piling[10].

2.2 Review of Current Approach

A non-exhaustive review of EIAs for offshore wind farms has found inconsistencies in relation to the level of detail given to piling noise. Many scope out its assessment, without providing any evidence to justify this position. The following section summarises how airborne noise from piling is assessed for those projects where a more detailed assessment was conducted, focusing on source level rather than propagation.

In one case, data measured for the installation of a monopile, 2.5 m in diameter, for a long-term meteorological mast are presented[11,12]. The assessment relies on the arithmetic average of measurements which leads to a calculated sound power level of 130 dB L_{wA}. No hammer energies are provided. The assessment acknowledges that the sound power level from piling will be higher than for the meteorological mast, but calculates that limits would be met provided sound power levels are ≤148 dB L_{wA}. There is significant scatter in the presented data, with the 95th percentile value resulting in a sound power level of 143 dB L_{wA}. This 95th percentile value corresponds with data presented by van Renterghem et al[13], which found a maximum sound power level of 145 dB L_{wA} for a pin pile with a diameter of 1.83m. For sake of comparison, BS 5228-1 includes comparable sound power levels for pin piles with a diameter of 34 cm[14].

In 2018, an assessment was conducted based on source levels of 139 dB L_{wA} provided by IQIP for their S-1200 hammer, with a maximum energy of 1,200 kJ[15,16]. The assessment scaled this value based on maximum hammer energy, with implied levels of up to 145 dB L_{wA} for hammer energies of 5,000 kJ. Various other EIAs include assumed levels which can be traced back to this

measurement[17,18,19], in some cases scaling based on maximum hammer energy, with source levels of 137 – 139 dB L_{wA} for hammer energies of 2,500 – 5,500 kJ.

None of the assessments reviewed factor in the radius of the pile or its exposed length above the water in determining source level. The former has been shown to be important in underwater noise assessments[20], while airborne sound measurements showed the latter was of greater importance than the hammer energy[7]. Arklow Bank Wind Park 2 project worked with a hammer manufacturer to determine assumed source levels of between 149 and 151 dB L_{wA} for hammer energies between 4,000 and 6,600 kJ[21]. These levels were based on a measurement of the same S-1200 hammer, which indicated source levels of 136 dB L_{wA} at approximately one-third of its maximum energy.

There is a spread of source levels assumed in EIAs, from 137 dB to 151 dB L_{wA} relating to hammer energies of between 2,500 kJ and 6,600 kJ. There is a lack of consistency regarding how data are interpreted and a need for more data to increase the robustness of assumed levels. In addition, where spectral data are presented there is little discussion about the influence of the design of the pile.

2.3 Analytical Model for Source Level

An approach to predict airborne noise from offshore piling is considered. A one-dimensional model for radial expansion of a pile due to its impact is translated from an underwater noise model presented in TNO's Aquarius 4 documentation[22]. Alongside the TNO model, a model of radiation efficiency has been adopted for a simple cylindrical shell to account for modes of the pile. This model assumes that noise radiated from the pile dominates, piling energy is evenly distributed over the pile diameter and that any underwater noise reradiated into the air is negligible.

2.3.1 One-Dimensional Model of Pile

The Aquarius 4 model considers the radial expansion of the pile wall due to the travelling axial compression wave and its reflections. The model is a first-order approximation in a one-dimensional model of the pile as an acoustic waveguide. This radial expansion creates an acoustic volume velocity adjacent to the pile. The model is summarised herein.

The surface area of the top of the pile, A_p is approximated based on the radius, a, and pile thickness, h, where $h<<a$. The axial wavenumber, k_p is calculated with respect to the angular frequency, ω, and the pile wavespeed, c_p, or with respect to the density of the pile, ρ_p, and its Young's modulus, E_p. The axial pile wall impedance, Z_p, is calculated with respect to A_p, ρ_p and c_p.

$$A_p(z) \approx 2\pi a(z)h, \qquad k_p = \frac{\omega}{c_p} = \omega\sqrt{\frac{\rho_p}{E_p}}, \qquad Z_p(z) = A_p(z)\rho_p c_p$$

The force, F, is calculated along the pile, z, with respect to the forcing function F_0, discussed in Section 2.3.2, and the pile length, L, terminated with impedance, Z_L, k_p and Z_p.

$$\hat{F}(\omega, z) = \hat{F}_0(\omega)\frac{Z_L \cos k_p\,(L-z) - jZ_p \sin k_p\,(L-z)}{Z_L \cos k_p\,L - jZ_p \sin k_p\,L}$$

This can be used to calculate the radial expansion, δ, where v_p is the Poisson's ratio. The source factor, as defined in ISO 18405:2016[23], can then be determined with respect to the density of the medium in which sound propagates, ρ_0.

$$\hat{\delta}(\omega, z) = \frac{v_p a\hat{F}(\omega, z)}{E_p A_p}, \qquad \hat{S}(\omega, z) = \frac{\rho_0 a\omega^2\hat{\delta}(\omega, z)}{2}$$

Based on the source factor, the time and spatially averaged sound power level ($L_{w,T}$, where T>>1min) can be calculated considering the length of the forcing function T_F (seconds), the blow rate b (blows per minute), the length of the exposed pile, l (m).

$$L_{w,T}(\omega) = 20\log_{10}\left(\frac{\overline{S_{rms}}(\omega)}{20\ \mu Pa}\right) + 10\log_{10}\left(\frac{T_F}{1\ s}\right) + 10\log_{10}\left(\frac{b}{60}\right) + 10\log_{10}(l)$$

The driveability assessment can be used to calculate the sound power level at multiple samples throughout the installation, from which an average of the whole pile driving event can be determined.

2.3.2 Forcing-Function

A forcing-function might be produced by the manufacturer of the hammer through finite element modelling, considering the driveability analysis and the design of the pile. While this would provide the most accurate forcing function, it is likely that this would only be produced for a small number of strikes of the pile.

Alternatively, a forcing function can be predicted analytically based on the driveability assessment, the pile design and the parameters of the impact hammer. Commonly used methods are Deeks & Randolph[24], Gavrilov's adaption to Deeks & Randolph[22] and Take et al 1999[25]. This analysis focusses on the Gavrilov's adaption due to its adoption in the Compile II workshop[26]. Reproduction of this model is beyond the scope of this paper but can be found in the Aquarius 4 documentation.

2.3.3 Radiation Efficiency

The radiation efficiency of the pile can also be modelled. By simplifying the pile into average radius and thickness, the model for acoustically thick cylindrical shells proposed by Wang and Lai[27] can be used, which incorporates work by Soedel[28]. Note that a shell is defined as acoustically thick when the ring frequency, f_r, is greater than the critical frequency, f_c.

$$f_r = \frac{1}{2\pi a}\sqrt{\frac{E_p}{\rho_p}}, \qquad f_c = \frac{{c_p}^2}{2\pi h}\sqrt{\frac{12\rho_p\left(1-{\nu_p}^2\right)}{E_p}}$$

Equations from Wang and Lai are supplemented by those required from Soedel in Appendix I for use. In reality, offshore piles tend to have varying diameters and thicknesses along their length. The validity of a simplified model should be tested, alongside the effects of it being driven and submersed.

2.3.4 Example Calculation

An example calculation has been carried out using a steel pile with a diameter of 10 m, thickness of 80 mm and total length 65 m with a total penetration depth of 25 m in water depth of 35 m. The assessment assumes a ram mass of 200 tonnes, anvil mass of 40 tonnes, cushion stiffness of 25 GN/m. The assessment considers a dummy driveability, shown in Figure 1, with a blow rate of 30 blows per minute and a slow start for 10 mins with 0.6 blows per minute. The model predicts a sound power level of 126 dB L_{wA} during the slow start, followed by a range of between 142 and 146 dB L_{wA} during the pile driving sequence, with the loudest period before reaching maximum hammer energy, due to the influence of the length of the exposed pile. The model predicts an energetic average of 145 dB L_{wA} over the entire pile driving event. The calculated spectrum is shown in Figure 1.

The predicted sound power level is within the range of those assumed at EIA stage. However, the spectrum displays a more significant roll-off at low frequencies than those presented in EIAs. In addition, the spectra presented in EIAs also tends to roll off at frequencies above approximately 1 kHz, which is not reproduced in this model, due to the dominance of the ω^2 factor. The predicted spectrum means that the radiation efficiency has an insignificant effect on total sound power level, although its effect could be of significance for long-range predictions.

More measured data are required to validate or discredit this model, and in particular to investigate whether the spectrum, dominated by the ω^2 factor, is realistic.

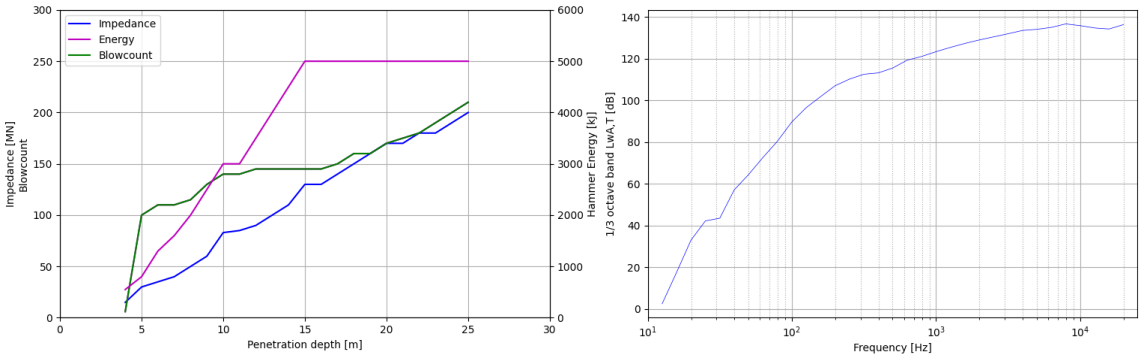

Figure 1: Example driveability (left) and calculated energetic average spectrum (right)

3 FOG SIGNALS

3.1 Introduction

It is required that audible fog signals are installed on offshore windfarms[8]. There are numerous examples of EIAs which include reference to these fog signals in their project descriptions[29,30], but the author has not found any examples of the sound from these installations being acknowledged in scoping or in the noise assessments. In a nod to this being the 50th anniversary of the Institute of Acoustics, the history of foghorn acoustics and the role of Trinity House to our modern understanding of acoustics, is celebrated. The potential for fog signals to result in adverse impact is discussed and a simple risk assessment tool is presented.

3.2 A Brief History of the Study of Foghorn Acoustics

Foghorns began to be installed around the UK from 1862[31]. In the 19th century and early 20th century, life-saving research into the propagation of sound over water was commissioned by Trinity House. The majority of research was conducted by two preeminent scientists, likely known to current-day acousticians, John Tyndall and Lord Rayleigh. The latter was particularly interested in the design of the horns, for example demonstrating that a narrower lateral expansion would result in a wider directivity, a fundamental concept widely familiar to modern-day acousticians.

Tyndall's efforts were largely concentrated on the propagation of sound over water. This was tested experimentally by triggering different types of fog signalling and having people on boats at different distances report on the audibility[32]. Tyndall made some important observations, such as increased audibility in foggy conditions, and broadly concluded that the specific atmospheric conditions were crucial to determining the audible distance of any signal. These experiments were shortly after Stokes' groundbreaking theory about wind shear and its effects on propagation[33], and Tyndall tentatively endorses this theory.

Looking at the experiments through a modern lens, it appears that anecdotal observations of meteorological conditions at ground height was likely responsible for some unexplained effects. However, other artefacts have been left unresolved, such as inexplicable reflections of the sound. Tyndall hypothesised that these were due to reflective acoustic clouds, a theory discredited shortly after. However, the observations bear a striking resemblance to unexplained effects recently discussed while presenting measurements of sound propagation over water[34] (although not included in the paper). Ultimately, the key finding from the experiments was the variability of sound propagation over such long distances. Trinity House addressed this by cautioning that "the mariner when he hears a fog signal, ought to assume the minimum rather than the maximum distance"[31].

While examples can be found of complaints of noise from foghorns[35,36,37], the research commissioned by Trinity House was focussed on improving the reliability of foghorns rather than reducing their potential impact. Renton hypothesises that the public's understanding of the importance of foghorns in the safety of shipping reduced the frequency of complaints[31]. Both the reliability of sending effective signals and any complaints could have been resolved if Trinity House had considered suggestions of using underwater signals. Despite this, over the years, foghorns were adopted locally as important soundmarks, with the public, in some cases, lamenting their eventual loss[38].

3.3 Offshore Windfarm Requirements

The Standard Marking Schedule for Offshore Installations[8] requires that offshore installations include an audible fog signal with a usual range of 2 nautical miles, calculated in accordance with the IALA guidance R0109[39]. The definition of usual range is the range at which a signal has a 50% chance of being heard on 50% of vessels during relatively calm conditions. As modern vessels emit a high proportion of low frequency sound, most modern fog signals operate between 600 and 900 Hz. The IALA Guidance determines the necessary source level depending on the system's frequency. While some aspects are not detailed in full, the calculation procedure in R0109 can be approximated, giving a relationship between minimum sound power level and frequency, shown in Figure 2 alongside the properties of various commercial systems. In the UK, fog signals must emit a 30 second pattern using morse letter U. A spectrogram of this is compared with historic foghorns in Figure 3.

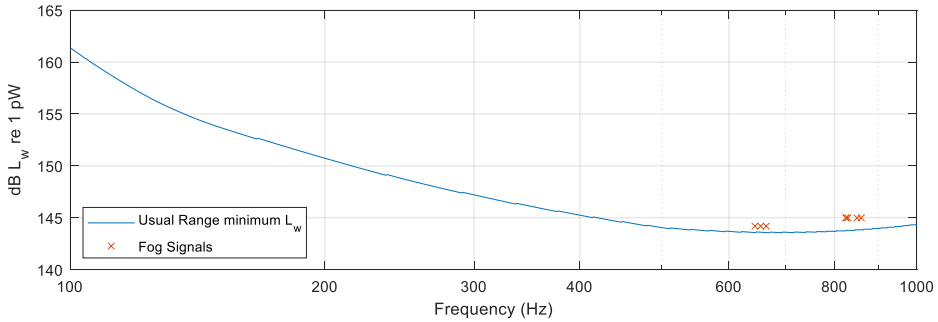

Figure 2: R0109 minimum sound power level and commercially available systems

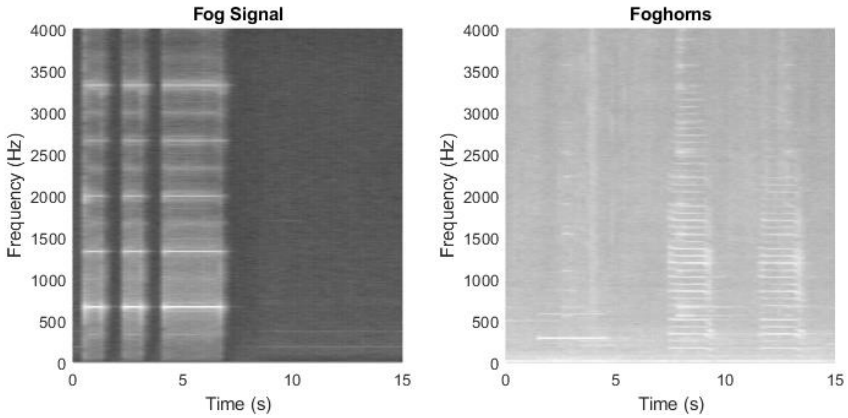

Figure 3: Spectrogram of modern fog signal (above) and two types of foghorn (below, diaphone: 0 – 5s, siren: 7 – 15s)

Considering the high sound power levels and the fact that advection fog can occur during windy conditions, with high windspeeds increasing the depth of the fog[40], there is a possibility of these high source levels combining with strong downward refracting conditions, resulting in the possibility of fog signals being audible at long distances. It should be noted that the author is unaware of any complaints relating to fog signals, and it is understood that modern-day complaints to Trinity House relate to onshore foghorns rather than offshore fog signals.

3.4 Fog Signal Risk Assessment Screening Tool

The relationship between sound power level and frequency defined by the 2 nm usual range requirement has been used to determine a simple risk assessment tool. The proposed tool makes use of the propagation method described in BEK135[6].

The tool assumes the impact would be determined using BS 4142:2014+A1:2019[41]. The signal is assumed to be subject to a -9 dB on-time correction, a 6 dB tonal correction and a 3 dB intermittency correction. No impulsivity would be expected at these distances. The tool considers the assessment relates to rural areas with relatively low background sound levels, assuming any signal with a rating level less than 30 dB would be of low risk, between 30 and 40 dB of medium risk and above 40 dB of high risk. The screening tool is shown in Figure 4.

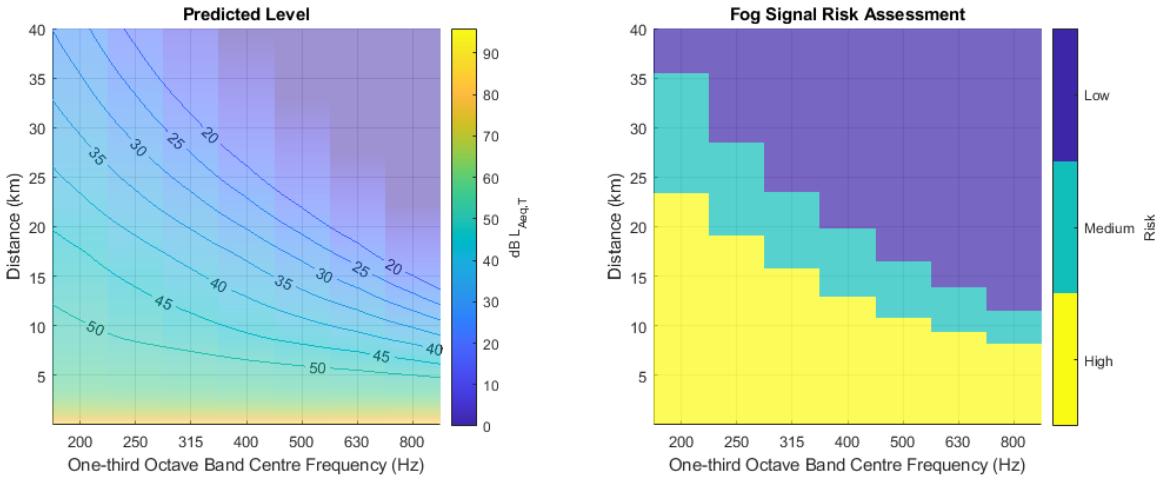

Figure 4: Proposed risk assessment tool for fog signal noise

4 CONCLUSIONS AND RECOMMENDATIONS

Source levels assumed for airborne sound from offshore piling are subject to a high degree of variability at the EIA stage. Many of the assumed levels stem from a single historic measurement, which is inconsistently interpreted and relates to a much smaller pile that those typically assessed for modern windfarms. An underwater noise model has been translated to the atmosphere for further investigation, although its adoption is not recommended until sufficient data is available for its validation. It is recommended that industry and/or academia conduct further measurements of this activity to validate analytical models or to develop empirical models.

The study of the acoustics of foghorns, largely funded by Trinity House, led to some foundational concepts underpinning our modern understanding of acoustics. While foghorns are no longer operated for safety purposes at lighthouses around the coast, fog signals are still required in UK water on manmade offshore structures. These fog signals require very high sound power levels, but the potential impact of these is not typically assessed in EIAs. A risk assessment tool is proposed based on the requirements in the UK which can be used to identify sites where more detailed assessment might be required.

Thanks to Sasha Gavrilov for providing the forcing-function code, John Caskey at Hydrosphere for fog signal recording, Alan Renton for the foghorn recordings and Jennifer Lucy Allan for foghorn info.

5 REFERENCES

1. The Crown Estate, “UK Offshore Wind Report 2023,” 2023.
2. DNV, “Energy Transition Outlook 2023 - A global and regional forecast to 2050,” 2023.

3. Wind Europe, “Offshore Wind in Europe - Key trends and statistics 2019,” 2019.
4. E. A. King and L. N. Bhraonáin, “Evaluating the potential impact of noise annoyance from offshore wind turbines in Ireland,” in Forum Acusticum 2023, Turin, 2023.
5. M. Bußе, K. Lowe, S. Broneske and S. Uchiyama, “Identifying and overcoming the challenges of offshore wind park noise in Japan,” in Inter.Noise 2023, Chiba, 2023.
6. Miljøministeriet, “BEK nr 135 af 07/02/2019 (Gældende): Bekendtgørelse om støj fra vindmøller,” 2019.
7. C. Birch and S. Stephenson, Predicting and assessing airborne noise from offshore piling of wind turbine foundations, 2021.
8. Department of Energy & Climate Change, “Standard Marking Schedule for Offshore Installations,” 2011.
9. J. Sims, “The assessment of noise from construction of offshore renewable energy infrastructure,” Acoustics Bulletin, vol. March/April 2017, pp. 46-53, 2017.
10. BBC, “Rampion wind farm: Offshore piling work wakes residents,” 21 07 2016. [Online]. Available: https://www.bbc.co.uk/news/uk-england-sussex-36857576. [Accessed 18 07 2024].
11. E.ON, “Rampion Offshore Wind Farm. ES Section 27 - Noise,” 2012.
12. E.ON, “Rampion Offshore Wind Farm. ES Section 27 - Noise. Appendices 27.2 - 27.3,” 2012.
13. T. Van Renterghem, L. Dekoninck and D. Botteldooren, “Propagation distance-of-concern for offshore wind turbine airborne sound during piling and normal operation,” in Forum Acusticum, Kraków, 2014.
14. BSI, “BS 5228-1:2009+A1:2014 - Code of practice for noise and vibration control on construction and open sites - Part 1: Noise,” 2014.
15. Vattenfall Wind Power Ltd, “Thanet Extension Offshore Wind Farm, Environmental Statement Volume 3, Chapter 10: Noise and Vibration,” 2018.
16. Vattenfall Wind Power Ltd, “Thanet Extension Offshore Wind Farm, Environmental Statement Appendix 10.2: Noise and Vibration Supporting Information,” 2018.
17. NISA - North Irish Sea Array, “Environmental Impact Assessment Report. Volume 5: Wider scheme aspects. Chapter 30: Noise and Vibration,” 2024.
18. Oriel Windfarm, “Environmental Impact Assessment Report - Volume 2C. Appendix 25-2: Noise Modelling Methodology,” 2024.
19. Awel y Môr Offshore Wind Farm, “Environmental Statement. Volume 3, Chapter 10: Noise and Vibration,” 2022.
20. J. von Pein, T. Lippert, S. Lippert and O. von Estorff, “Scaling laws for unmitigated pile driving: Dependence of underwater noise on strike energy, pile diameter, ram weight, and water depth,” Applied Acoustics, vol. 198, 2022.
21. SSE Renewables, “Arklow Bank Wind Part 2 - Environmental Impact Assessment Report. Volume II. Chapter 8: Airborne Noise,” 2024.
22. C. de Jong, B. Binnerts, M. Prior, M. Colin, M. Ainslie, I. Mulder and I. Hartstra, “Wozep – WP2: update of the Aquarius models,” 2019.
23. BSI, “BS ISO 18405:2017 Underwater Acoustics - Terminology,” BSI, 2017.
24. A. J. Deeks and M. F. Randolph, “Analytical modelling of hammer impact for pile driving,” International Journal for Numerical and Analytical Methods in Geomechanics, vol. 17, no. 5, pp. 279-302, 1993.
25. W. A. Take, A. J. Valsangkar and M. F. Randolph, “Analytical solution for pile hammer impact,” Computers and Geotechnics, vol. 25, pp. 57-74, 1999.
26. T. Lippert, M. Ruhnau, S. Lippert, O. von Estorff, M. A. Ainslie and M. Nijhof, “COMPILE II: A real-life benchmark scenario for pile driving noise estimations,” in UACE2017 - 4th Underwater Acoustics Conference and Exhibition, Skiathos, 2017.
27. C. Wang and J. C. S. Lai, “The sound radiation efficiency of finite length acoustically thick circular cylindrical shells under mechanical excitation I: Theoretical analysis,” Journal of Sound and Vibration, vol. 232, no. 2, pp. 431-447, 2000.
28. W. Soedel, Vibrations of Shells and Plates. Third Edition, revised and expanded, 2004.
29. Moray West Offshore Windfarm, “Offshore EIA Report - Chapter 1 Introduction,” 2018.
30. Berwick Bank Wind Farm, “Offshore Environmental Impact Assessment - Appendix 27: Outline Lighting and Marking Plan”.

31. A. Renton, Lost Sounds - The story of coast fog signals, Dunbeath: Whittles Publishing, 2001.
32. J. Tyndall, Sound, Third ed., London: Longmans, Green, and Co, 1875.
33. G. G. Stokes, “On the effect of wind on the intensity of sound,” in Report of the Twenty-seventh Meeting of the British Association for the Advancement of Science; held at Dublin in August and September 1857: Notices and Abstracts of Miscellaneous Communications to the Sections., 1858.
34. E. Thysell, R. Egedal, L. S. Søndergaard, C. Thomsen, T. Sørensen and F. Bertagnolio, “High resolution analysis of measurements, and comparison of models for long distance noise propagation over water for an elevated height-adjustable sound source,” in 10th International Conference on Wind Turbine Noise, Dublin, 2023.
35. R. W. Munro, Scottish Lighthouses, Stornoway: Thule, 1979.
36. J. Lucy Allan, “The Lizard & The Cloch - Time and Place in 19th century foghorn installations,” in Invisible Places, São Miguel, 2017.
37. T. Hecker, “The era of megaphonics: On the productivity of loud sound, 1880-1930,” 2014.
38. J. Lucy Allan, The Foghorn's Lament - The disappearing music of the coast, London: White Rabbit, 2022.
39. IALA, “R0109 (E-109) The calculation of the range of a sound signal,” Saint Germain en Laye, 1998.
40. National Oceanic and Atmospheric Administration, “Fog Types,” n.d..
41. BSI, “BS 4142:2014+A1:2019 - Methods for rating and assessing industrial and commercial sound,” BSI, 2019.
42. Wolfram MathWorld, “Hankel Function of the Second Kind,” [Online]. Available: https://mathworld.wolfram.com/HankelFunctionoftheSecondKind.html. [Accessed 18/07/2024].

6 APPENDIX I – RADIATION EFFICIENCY

The formulas of Wang and Lai[27] and Soedel[28] have been collated concisely for use. Further explanation and derivation can be found in the referenced texts. The referenced texts allow for the calculation of longitudinal, axial and flexural vibrations. In Wang and Lai’s example, it is assumed that flexural vibrations dominate, and the other two modes are ignored. In the use-case of impact driving of offshore monopiles, the monopile is struck from the head, and it is therefore assumed that longitudinal waves dominate, i.e. $F_z = 1$, $F_\theta = F_r = 0$, only calculating for $i = 1$.

$$D = \frac{E_p h^3}{12\left(1 - {\nu_p}^2\right)}, \qquad K = \frac{E_p h}{1 - {\nu_p}^2}, \qquad k_{zm} = \frac{m\pi}{L} - \frac{\pi}{2L}, \qquad k_{\theta n} = \frac{n}{a}$$

$${\omega_{m,n}}^2 = \frac{D}{\rho h}\left({k_{zm}}^2 + {k_{\theta n}}^2\right)^2 + \frac{K\left(1 - {\nu_p}^2\right)}{\rho h a^2} \cdot \frac{{k_{zm}}^4}{\left({k_{zm}}^2 + {k_{\theta n}}^2\right)}$$

$$\sigma_{m,n}(\omega) = \int_{-k}^{k} \frac{2kl}{\pi^2 a {k_r}^2 \left|\frac{\mathrm{d}H_n^{(2)}(k_r a)}{\mathrm{d}(k_r a)}\right|^2} \left(\frac{m\pi/L}{k_z + m\pi/L}\right)^2 \frac{\sin^2\left(L/2(k_z - m\pi/L)\right)}{\left(L/2(k_z - m\pi/L)\right)^2} \mathrm{d}k_z$$

Where k_r is shown below, alongside the derivative of a Henkel function of the second kind[42]:

$$k_r = \sqrt{k^2 - {k_z}^2}, \qquad \frac{\mathrm{d}H_n^{(2)}(z)}{\mathrm{d}z} = \frac{1}{2}\left(H_{n-1}^{(2)}(z) - H_{n+1}^{(2)}(z)\right)$$

$$k_{11} = K\left(\left(\frac{m\pi}{L}\right)^2 + \frac{1-\nu}{2}\left(\frac{n}{a}\right)^2\right), \qquad k_{12} = k_{21} = K\frac{1+\nu}{2} \cdot \frac{m\pi}{L} \cdot \frac{n}{a}, \qquad k_{13} = k_{31} = \frac{\nu K}{a} \cdot \frac{m\pi}{L},$$

$$k_{22} = \left(K + \frac{D}{a^2}\right)\left(\frac{1-\nu}{2}\left(\frac{m\pi}{L}\right)^2 + \left(\frac{n}{a}\right)^2\right), \qquad k_{23} = k_{32} = -\frac{K}{a} \cdot \frac{n}{a} - \frac{D}{a} \cdot \frac{n}{a}\left(\left(\frac{m\pi}{L}\right)^2 + \left(\frac{n}{a}\right)^2\right),$$

$$k_{33} = D\left(\left(\frac{m\pi}{L}\right)^2 + \left(\frac{n}{a}\right)^2\right)^2 + \frac{K}{a^2}$$

$$a_1 = -\frac{1}{\rho h}(k_{11} + k_{22} + k_{33}), \qquad a_2 = \frac{1}{(\rho h)^2}\left(k_{11}k_{33} + k_{22}k_{33} + k_{11}k_{22} - {k_{23}}^2 - {k_{12}}^2 - {k_{13}}^2\right)$$

$$a_3 = \frac{1}{(\rho h)^3}\left(k_{11}{k_{23}}^2 + k_{22}{k_{13}}^2 + k_{33}{k_{12}}^2 + 2k_{12}k_{23}k_{13} - k_{11}k_{22}k_{33}\right)$$

$$\alpha = \cos^{-1}\left(\frac{27a_3 + 2{a_1}^3 - 9a_1a_2}{2\sqrt{({a_1}^2 - 3a_2)^3}}\right), \qquad \zeta_{mn} = \frac{\lambda}{2\rho h\omega_{mn}}$$

$${\omega_{mn1}}^2 = -\frac{2}{3}\sqrt{{a_1}^2 - 3a_2}\cos\frac{\alpha}{3} - \frac{a_1}{3}$$

$$\frac{A_{mn1}}{C_{mn1}} = -\frac{k_{13}(\rho h{\omega_{mn1}}^2 - k_{22}) - k_{12}k_{23}}{(\rho h{\omega_{mn1}}^2 - k_{11})(\rho h{\omega_{mn1}}^2 - k_{22}) - {k_{12}}^2}$$

$$\frac{B_{mn1}}{C_{mn1}} = -\frac{k_{23}(\rho h{\omega_{mn1}}^2 - k_{11}) - k_{21}k_{13}}{(\rho h{\omega_{mn1}}^2 - k_{11})(\rho h{\omega_{mn1}}^2 - k_{22}) - {k_{12}}^2}$$

$$U_{zmn1} = \frac{A_{mn1}}{C_{mn1}}\cos\frac{m\pi z}{L}\cos n\theta\,, \qquad U_{\theta mn1} = \frac{B_{mn1}}{C_{mn1}}\sin\frac{m\pi z}{L}\sin n\theta\,, \qquad U_{rmn1} = \sin\frac{m\pi z}{L}\cos n\theta$$

$$N_{mn1} = \int_0^L\int_0^{2\pi}\left({U_{zmn1}}^2 + {U_{\theta mn1}}^2 + {U_{rmn1}}^2\right)a\mathrm{d}\theta\mathrm{d}z$$

$$F_{mn1} = \frac{1}{\rho hN_{mn1}}\int_0^L\int_0^{2\pi}(F_zU_{zmn1} + F_\theta U_{\theta mn1} + F_rU_{rmn1})\,a\mathrm{d}\theta\mathrm{d}z$$

$$\bar{\sigma}(\omega) = \frac{\sum_m^\infty\sum_n^\infty(\sigma_{mn}(\omega)|F_{mn1}|^2N_{mn1})/\left((\omega_{mn}{}^2 - \omega^2)^2 - 4\zeta_{mn}{}^2\omega_{mn}{}^2\omega^2\right)}{\sum_m^\infty\sum_n^\infty(|F_{mn1}|^2N_{mn1})/\left((\omega_{mn}{}^2 - \omega^2)^2 - 4\zeta_{mn}{}^2\omega_{mn}{}^2\omega^2\right)}$$